Magnetic-Field Induced Strains in Ferromagnetic Shape Memory Alloy $Ni_{55}Mn_{23}Ga_{22}$ Deposited by RF-Magnetron Sputtering

Florent Bernard,* Christophe Rousselot, Patrick Delobelle, Laurent Hirsinger, Pierre Burdet

1.5 μm–$Ni_{55}Mn_{23}Ga_{22}$ ferromagnetic thin films were deposited onto silicon substrates and silicon single beam cantilever using radio-frequency magnetron sputtering. As-deposited sample and heat-treated thin films were studied on their silicon substrates and peeled off to determine the influence of the stress. Post-heat treatment process allows at the films to achieve the shape memory effect (SME). Vibrating sample magnetometer (VSM) and deflection measurement of the sample annealed at 873 K during 36 ks exhibit ferromagnetic martensitic structure with a typical SME response to the magnetic field induced strains which match the values of the bulk material.

Introduction

The near-stoichiometric Ni_2MnGa ferromagnetic alloys are one of these smart materials, that show a great interest when they are deposited as thin films by radio-frequency (rf) sputtering. These films of shape memory alloys (SMAs) are prospective materials for micro and nanosystem applications.[1–4] Thanks to the various ways to activate this material,[5] it can be incorporated in novel actuator, sensor and magnetic micro or nanosystems, as thin films in free-standing form[6] or attached to the substrate.[7] However, the properties of the SMAs polycrystalline thin films depend strongly on their structure and internal stress, which are developed during the sputtering process and also during the post-deposition annealing treatment.[6,8–11] In this way, $Ni_{55}Mn_{23}Ga_{22}$ — rf sputtered thin films were elaborated to study the influence of the process on their magnetic field induced strains (MFIS). Their composition, crystallographic structure, internal stress, indentation modulus, hardness and deflection induced by magnetic field were systematically studied as a function of the temperature of silicon substrate and of the annealing treatment. In addition, the temperature dependencies on mechanical properties such as mean stress, roughness, and hardness and indentation modulus were measured and correlated to crystal structure and morphology changes.[12,13] Also, in previous study, it was shown that the silicon do not diffuse during annealing treatment.[14]

In the present work, we compare the MFIS of the samples between as-deposited and annealed during 36 ks at 873 K. The accurate measurements of interatomic spacing d in the normal direction of the film were carried out for various constant temperatures in order to correlate d with the martensitic transformation (T_m) and with the properties exhibited by the Ni–Mn–Ga/Si film (supported film). Vibrating sample magnetometer (VSM) and magnetostrain measurements were performed to obtain the thermo magnetic and MFIS properties of these Ni–Mn–Ga/Si films. Thermal analysis and MFIS are also carried out on freestanding films allowing to observe giant displacement for the 1.5 μm–36 ks–873 K–$Ni_{55}Mn_{23}Ga_{22}$ film.

F. Bernard, C. Rousselot
Dept MN2S, 4 Place Tharradin, BP 71427, Institut FEMTO-ST (UFC/CNRS/ENSMM/UTBM), 25211 Montbéliard, France
E-mail: florent.bernard@pu-pm.univ-fcomte.fr
P. Delobelle, L. Hirsinger
Dept MN2S, 24 Chemin de l'Epitaphe, Institut FEMTO-ST (UFC/CNRS/ENSMM/UTBM), 25000 Besançon, France
P. Burdet
CIME-EPFL, Bat MXC-134, Station 12, 1015 Lausanne, Switzerland

Plasma Process. Polym. **2009**, *6*, S822–S825

DOI: 10.1002/ppap.200932104

Experimental Part

The preparation and the basic characterization of the films were described elsewhere.[13] As-deposited and annealed 36 ks–873 K samples sputtered at 120 W and at argon pressure of 1 Pa have a chemical composition of $Ni_{55}Mn_{23}Ga_{22}$. In order to perform thermal and magnetostrain analysis freestanding films are prepared. Silicon substrates are removed by KOH solution (10 M at 363 K) which attacks selectively the composite until complete dissolution of the silicon.

The accurate measurements of the peak position in function of temperature were carried out by X-ray diffraction (XRD) with a PANalytical X'Pert Pro with a detector X'Celerator from $2\theta = 40^\circ$ to $2\theta = 50^\circ$. The step and the integration time were 0.008° and 100 s/step, respectively. To control the temperature analysis, samples were put in a specific heating-cooling chamber under a constant flow rate of helium. Therefore shifting of the planar spacing d can be extracted of the XRD experiment to determine the coefficient of thermal expansion (CTE). In addition the size of the structural domain, also called the "nanocrystal dimension" L is routinely extracted from of the peak half-width and using the standard Scherrer formula. All the measurements and results were operating with Philips specific software. Thermal analyses were carried out on freestanding films to determine T_m and Curie temperature (T_C). A differential scanning calorimeters (DSC) Mettler Toledo DSC 821 apparatus was used with Pt crucible of 150 μL under a constant flow rate 60 mL/min of argon to determine T_m of the films. Four cycles from 273 to 473 K at 10 K/min were performed to make sure of the measurement reproducibility. The remarkable Curie point temperature was determined by thermo gravimetric analysis (TGA) TA instruments TGA Q50 under magnetic field. Indeed, a magnet was put under the crucible containing peeled-off films. To correlate magnetostrain measurement to typical magnetic properties, saturation magnetization, remanent magnetization, coercive force (H_c), and susceptibility (χ), the VSM in function of the sample temperature were studied. For theses studies realized on the Ni–Mn–Ga/Si film, the applied magnetic field was ranged between −4 and 4 T and the temperature experiment was droved from 10 to 298 K. MFIS was measured on the peeled-off films and supported films by qualitative and quantitative experiments, respectively. The peeled-off films prepared as embed beams were observed with classical optical device with and without magnetic field of 200 kA/m. The magnetostrain on the supported films were carried out by an experimental device with whom the deflections were measured at the beams end with an optical probe MTI 2000 Fotonic sensor with a 2032 RX probe. For this characterization, the magnetic field was produced by an electromagnet BRUCKER BE 20 C 8 fed with a power supply BLMPS 90/30 UCM2, and was measured with a Hall effect probe BELL 6010.

Results and Discussion

Changes of Lattice Parameter

The accurate XRD measurements on the as-deposited sample in the range from 298 to 473 K show a slight linear shift of the diffraction peak, $2\theta = 43.874^\circ$ and $2\theta = 43.653^\circ$, respectively. The shape of the peak seems to remain the same without widening or narrowing at half-width height. The peak position near the position of the characteristic austenitic peak tends to associate the present phase to the austenitic phase. However, the asymmetry and the width of the peak, add to the preliminary selected area electron diffraction (SAED) obtained by transmission electron microscopy (TEM), show a very large polycrystalline structure of martensitic small grain randomly distributed.[13] Microstructure of the cross-section is composed of fine column composed of stacking small grains spaced by 2.063 Å. The annealed sample exhibit changes in its crystallographic structure and in the temperature dependencies. We can observe three different behaviors that a result of the martensitic transformation. Indeed the position of the peak for the XRD measurement performed at 298 K was observed at $2\theta = 44.539^\circ$. According to Chernenko et al.[2,8,11,16] this peak correspond to the martensitic tetragonal phase. Thanks to these XRD results, d and L were extracted from the peak position and from the half-width peak, respectively (Figure 1). The experimental dependency of the planar spacing $d(T)$ in the martensitic phase ($T < 420$ K) were divided in two parts, corresponding to paramagnetic (370–420 K) and ferromagnetic (300–360 K) states of the sample, and drawn two straight lines as shown in Figure 1. A change in the slope of the $d(T)$ curve at the Curie temperature is in agreement with dilatometric results reported for the Ni–Mn–Ga bulk alloys.[15] The more pronounced decrease of $d(T)$ in the ferromagnetic phase may be explained by the negative sign of the isotropic magnetoelastic constant[16] and softening of the elastic modulus in the vicinity of the T_m. Therefore from 370 to 420 K the CTE of the paramagnetic martensitic phase is $15 \pm 1 \times 10^{-6}\,K^{-1}$. At lower temperature the d shifting corresponds to the behavior of martensitic ferromagnetic phase with a CTE of $33 \pm 1 \times 10^{-6}\,K^{-1}$ in agreement with the bulk The CTE of the austenitic present phase is $18 \pm 1 \times 10^{-6}\,K^{-1}$ which match well the bulk value. Martensitic transformation also results in the temperature dependence of the L parameter. Anomalies in the $L(T)$ dependencies were produced by the reverse transformation as in the case of the lattice parameter. To conclude, $d(T)$ and $L(T)$ of the annealed sample at 873 K during 36 ks show the effect of the martensitic transformation which occur between 370 and 420 K.

Magnetic Properties

Magnetization curves $M(H)$ of the as-deposited sample (Figure 2) registered up to 4 T, remain dependent of the applied magnetic field with small value of magnetization (M) 0.040 T characteristic of non-saturating behavior. Remanent magnetization and susceptibility is also negligible even at very low temperature of 10 K, 0.009 T, and $0.2 \times 10^{-5}\,T \cdot A/m$, respectively. This typical behavior

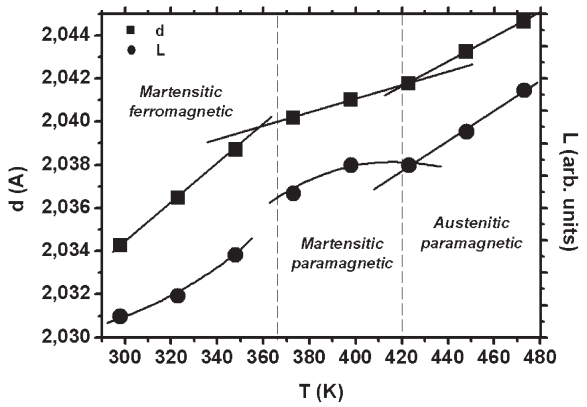

Figure 1. Temperature dependencies of the annealed 36 ks–873 K–$Ni_{55}Mn_{23}Ga_{22}$ sample, the planar spacing *d* (square) and the *L* parameter (round) are extracted by analysis of the peak position and the half-width of the diffraction peak, respectively. Vertical dashed lines border three temperature domains which correspond to martensitic ferromagnetic, martensitic paramagnetic, and austenitic paramagnetic phases. Straight line between square points represents the different coefficient of thermal expansion (CTE), curve lines between round points are visual guide for variation of the *L* parameter.

shows the non-ferromagnetic feature of the as-deposited sample. In contrast, magnetic response of the annealed sample depicted in Figure 2 reach a very high value of magnetization, with field of 0.4 T. The magnetization reaches 0.701 T which correspond to 93% of the saturation magnetization (M_s). Appearance of the ferromagnetic hysteresis and the large increase of the susceptibility show the spectacular effect of the annealing on the occurrence of the magnetic domains in the annealed films.

According to the crystallographic results, energy produce by the annealing treatment at 873 K during 36 ks allow a rearrangement of the microstructure that evolves from columnar to large grain of martensitic variants made up of magnetic domain.[13]

Magnetic Field Induced Strains

Considering the magnetic properties of this two kind of sample, quantitative studies on the film strain induced by magnetic field were made only on annealed and the supported films. Measurements under in-plane and out-plane applied magnetic field were performed on Si beam cantilevers and reported in Figure 3. Deflection shows a linear dependency with applied magnetic field, the response of this sample under in-plane magnetic field is three times higher than out-plane applied field. The magnetocrystalline anisotropy approaches the behavior of the bulk single crystals and high thickness thin films where the "easy-axis" was found to be in plane while the "hard-axis" was observed along the film normal. The out-of-plane magnetic anisotropy of Ni–Mn–Ga films was caused by the competitive contributions of the magnetocrystalline, stress induced and magnetostatic anisotropies.

Finally, in order to illustrate the capability of the annealed treatment to provide magneto-active films, as-deposited films (at 298 K) and annealed films (at 873 K during 36 ks) were peeled-off and compared by qualitative method. The films were exposed to the magnetic field created by a small magnet put on the top of the two right pictures. Without a magnetic field in the left pictures, the freestanding films remain wound and only the heat-treated film unwinds under an in-plane magnetic field of about[13] 200 kA/m. These good ferromagnetic properties of films match well with the structural and magnetic behavior observed on supported films (Figure 4).

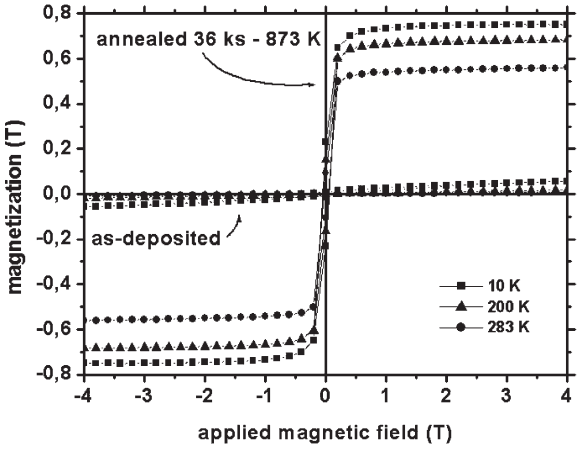

Figure 2. Magnetization curves under applied magnetic field in function of temperature for as-deposited sample and annealed 36 ks–873 K sample (mark with arrows). Square, triangle, and round represent measurements recorded at 10, 200, and 283 K, respectively.

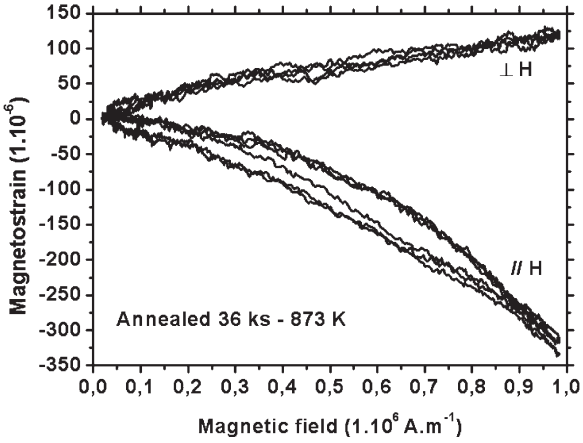

Figure 3. Magnetostrain curves under in-plane and out-plane magnetic field for the annealed 36 ks–873 K sample.

DOI: 10.1002/ppap.200932104

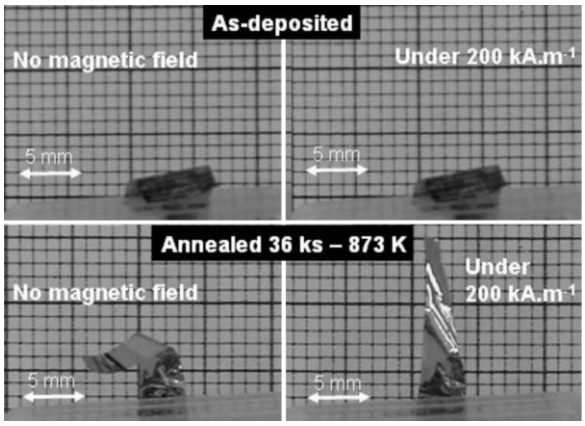

Figure 4. Film winding and unwinding under the action of a magnet placed on top of the two right pictures: Comparison of as-deposited film at 298 K and annealed one at 873 K for 36 ks.

Conclusion

Sputtered $Ni_{55}Mn_{23}Ga_{22}$ thin films must be heat treated to achieve shape memory properties. Martensitic transformation and magnetic behavior were not found on as-deposited sample without annealing. On the annealed ones, the planar spacing *d* and the nanocrystal dimension *L* exhibit temperature dependencies that matches well with the shape memory materials. This behavior of the annealed film remain the same that this one found in bulk materials, where the crystallographic changes induced by martensitic transformation can be ranged in various "class behavior" such as ferromagnetic martensitic, paramagnetic martensitic, and paramagnetic austenitic. They are bounded by the Curie and the martensitic transformation temperature in the range from 370 to 420 K.

Magnetic properties of the sample annealed at 873 K during 36 ks were improved, the widening process of the grain size allow developing magnetic domains. Typical response of the ferromagnetic materials was encountered with this sample, as a high magnetization under low applied field and a characteristic ferromagnetic hysteresis. The film strain induced by magnetic field show magnetocrystalline anisotropy with the easy axis oriented in the film plane. Quantitative and qualitative measurements on supported and freestanding films demonstrate a considerable magnetic actuation, which make 873 K–36 ks-annealed films very promising materials to be incorporated in novel actuator as microelectromechanical systems (MEMS).

Received: October 2, 2008; Accepted: April 19, 2009; DOI: 10.1002/ppap.200932104

Keywords: annealing; microelectromechanical systems (MEMS); Ni_2MnGa; physical vapor deposition (PVD); thin films

[1] S. A. Wilson, R. P. J. Jourdain, Q. Zhang, R. A. Dorey, C. R. Bowen, M. Willander, Q. U. Wahab, M. Willander, S. M. Al-hilli, O. N. Quandt, C. Johansson, E. Pagounis, M. Kohl, J. Matovic, B. Samel, W. v. d. Wijngaart, E. W. H. Jager, D. Carlsson, Z. Djinovic, M. Wegener, C. Moldovan, R. Iosub, E. Abad, M. Wendlandt, C. Rusu, K. Persson, *Mater. Sci. Eng. R.* **2007**, *56*, 1.
[2] V. A. Chernenko, S. Besseghini, *Sensors Actuators A* **2008**, *142*, 542.
[3] M. Kohl, D. Brugger, M. Ohtsuka, T. Takagi, *Sensors Actuators A* **2004**, *114*, 445.
[4] M. Kohl, D. Brugger, M. Ohtsuka, B. Krevet, *Sensors Actuators A* **2007**, *135*, 92.
[5] K. Ullakko, J. K. Huang, C. Kantner, R. C. O'Handley, V. V. Kokorin, *Appl. Phys. Lett.* **1996**, *69*, 1966.
[6] M. Ohtsuka, M. Sanada, M. Matsumoto, K. Itagaki, *Mater. Sci. Eng. A* **2004**, *378*, 377.
[7] H. Rumpf, C. M. Craciunescu, H. Modrow, K. Olimov, E. Quandt, M. Wuttig, *J. Magnetism Magn. Mater.* **2006**, *302*, 421.
[8] V. Chernenko, M. Kohl, S. Doyle, P. Mullner, M. Ohtsuka, *Scripta Materialia* **2006**, *54*, 1287.
[9] S. K. Wu, K. H. Tseng, J. Y. Wang, *Thin Solid Films* **2002**, *408*, 316.
[10] C. Liu, W. Cai, X. An, L. X. Gao, Z. Y. Gao, L. C. Zhao, *Mater. Sci. Eng. A* **2006**, *438–440*, 986.
[11] V. A. Chernenko, M. Ohtsuka, M. Kohl, V. V. Khovailo, T. Takagi, *Smart Mater. Struct.* **2005**, *14*, S245.
[12] F. Bernard, C. Rousselot, L. Hirsinger, P. Delobelle, *Plasma Process. Polym.* **2007**, *4*, S846.
[13] F. Bernard, P. Delobelle, L. Hirsinger, C. Rousselot, *Mater. Sci. Forum* **2008**, *583*.
[14] F. Bernard, C. Rousselot, L. Hirsinger, P. Delobelle, *Eur. Phys. J.* **2008**, *158*, 187.
[15] V. V. Kokorin, V. A. Chernenko, E. Cesari, J. Pons, C. Segui, *J. Phys: Condens Mat.* **1996**, *8*, 6457.
[16] V. A. Chernenko, V. A. L'vov, M. Pasquale, C. P. Sasso, S. Besseghini, D. A. Polenur, *Int. J. Appl. Electromagn. Mech.* **2000**, *12*, 1.